Electronic Supplementary Material (ESI) for Journal of Materials Chemistry C.

Supplementary Information for

Van der Waals 2D Metallic Materials for Low-Resistivity Interconnects

Yaoqiao Hu, Patrick Conlin, Yeonghun Lee, Dongwook Kim, and Kyeongjae Cho

Department of Materials Science and Engineering, The University of Texas at Dallas, Richardson, Texas 75080, USA

Corresponding Author: Kyeongjae Cho (kjcho@utdallas.edu)

Table S1 Calculated figure of merit ρλ ($\times 10^{-16}$ Ω·m^2), for 2D metallic TMDs comprised of various transition metals and chalcogen elements. Both 1T and 2H phases are considered and presented as 1T/2H. Materials with a ρλ value higher than 100×10^{-16} Ω·m^2 are considered semiconductors and denoted with a -.

	Ti	Zr	Hf	V	Nb	Ta	Mo	W	Re	Pd	Pt
S	91.7/-	-/-	-/-	12.9/13.6	10.3/12.1	10.8/13.5	20.6/-	17.6/-	10.0/22.9	-/99.3	-/29.8
Se	29.8/-	-/-	-/-	11.9/13.7	11.7/13.4	12.0/13.5	30.9/-	25.4/-	10.9/23.9	18.4/19.7	-/20.4
Te	17.1/56.0	27.5/86.0	32.1/97.6	13.2/13.9	12.3/15.2	11.6/14.5	75.3/-	43.0/-	12.4/16.5	18.1/26.5	25.9/20.1

Table S2 Calculated figure of merit ρλ ($\times 10^{-16}$ Ω·m^2), for 2D metallic M_2AX comprised of various transition metals and group 13/14 elements. Both carbides (X=C) and nitrides (X=N) are considered and presented as C/N.

	Ti	V	Zr	Hf	Ta	Mo	Cr
Al	11.5/13.8	9.68/9.59	11.4/12.9	10.9/12.1	9.24/19.4	8.09/6.84	7.45/8.38
Si	12.7/10.2	12.3/7.54	12.8/8.85	12.2/8.50	14.4/9.26	8.57/6.51	8.92/11.8
Ge	12.3/8.56	9.59/7.28	12.5/7.90	11.7/7.72	13.4/10.5	8.62/7.02	8.37/11.4
Ga	11.9/17.3	10.2/8.12	11.3/16.9	11.2/12.8	9.39/13.7	7.10/5.25	7.83/6.97
In	12.6/19.1	12.0/8.67	12.5/18.3	12.3/16.3	10.4/8.94	6.66/8.27	7.06/8.82
Sn	9.08/7.17	7.39/6.74	10.2/7.74	9.25/7.60	7.76/7.13	7.73/10.7	7.56/11.1

Table S3 Calculated figure of merit ρλ ($\times 10^{-16}$ Ω·m^2), for 2D metallic M_3AX_2 comprised of various transition metals and group 13/14 elements. Both carbides (X=C) and nitrides (X=N) are considered and presented as C/N.

	Ti	V	Zr	Hf	Ta	Mo	Cr
Al	16.0/17.3	13.7/9.72	15.1/22.7	15.3/22.2	109/19.2	7.77/7.14	7.91/7.98
Si	17.2/29.0	11.8/8.32	14.6/18.4	13.5/17.2	21.8/15.3	8.90/5.92	8.05/9.79
Ge	17.4/17.6	9.39/8.37	15.3/16.8	14.2/15.9	15.5/11.9	8.34/9.62	8.22/11.4
Ga	14.7/17.1	12.7/9.37	14.5/20.4	14.6/20.2	91.1/8.97	8.34/7.65	7.63/8.28
In	17.0/16.7	12.1/10.5	15.7/22.1	15.9/21.8	94.6/8.79	8.40/12.4	7.52/10.9
Sn	17.0/13.4	9.33/8.29	16.5/18.1	16.4/17.7	13.3/8.86	8.81/18.0	9.17/17.8

Table S4 Calculated figure of merit ρλ ($\times 10^{-16}$ Ω·m^2), for 2D metallic M_4AX_3 comprised of various transition metals and group 13/14 elements. Both carbides (X=C) and nitrides (X=N) are considered and presented as C/N.

	Ti	V	Zr	Hf	Ta	Mo	Cr
Al	20.1/102	21.6/9.58	20.6/42.0	21.1/31.3	19.3/12.8	9.83/6.50	10.0/11.0
Si	19.3/16.4	12.8/9.61	16.6/13.7	15.7/12.7	18.2/14.7	11.7/5.79	11.6/9.68
Ge	20.2/16.8	12.2/9.21	17.2/13.6	16.3/13.0	13.6/12.4	12.0/11.0	11.6/22.7
Ga	18.6/85.8	18.6/9.39	18.9/31.8	19.2/28.4	18.2/12.8	10.1/6.13	9.53/23.7
In	19.6/58.2	21.6/9.77	19.6/62.9	19.4/58.5	20.0/12.0	10.7/16.9	10.7/23.1

Sn	19.3/17.0	12.5/9.71	18.3/13.7	18.4/13.0	11.8/12.3	11.5/20.6	13.4/20.4

Table S5 Calculated figure of merit ρλ ($\times 10^{-16}\ \Omega \cdot m^2$), for 2D metallic metal oxides MOX comprised of various transition metals and chalcogen elements/-OH group. Since MOX has a rhombohedral structure, we present their in-plane resistivities in two directions: [100]/[010].

	Ti	V	Cr	Mn	Fe	Ce	Gd	U	Np	Pu
F	43.0/9.08	16.0/9.50	10.6/13.4	11.3/10.2	21.9/8.66	23.4/14.3	51.1/25.2	18.5/9.34	2.6/17.6	-
Cl	20.2/9.47	15.6/9.82	12.3/8.07	11.6/6.24	30.0/6.57	24.1/15.4	-	22.8/9.61	15.4/9.29	11.1/11.1
Br	26.0/9.42	20.8/9.61	17.0/7.38	9.23/8.68	39.2/6.21	25.6/14.8	-	18.7/9.56	15.6/9.35	8.64/8.45
I	37.9/11.8	20.7/12.3	16.3/12.0	9.95/8.33	41.6/4.84	29.8/14.2	-	14.4/9.34	19.6/9.28	-
OH	33.0/6.20	10.6/6.26	8.28/8.86	12.0/6.14	22.2/6.26	13.0/8.29	-	12.5/8.37	24.2/22.5	12.0/9.58

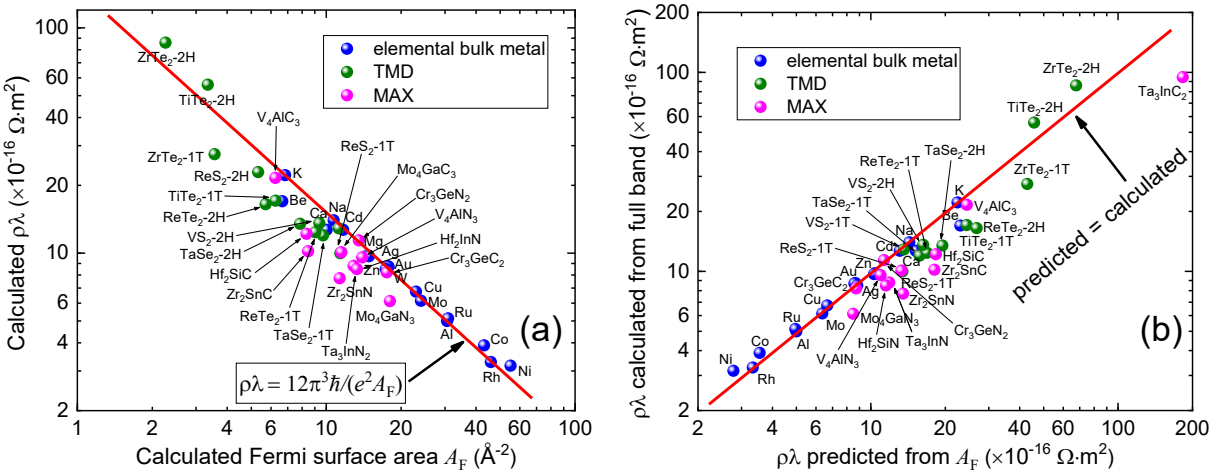

Figure S1. (a) Calculated ρλ versus calculated Fermi surface area A_F. The data points closely follow the $\rho\lambda = 12\pi^3\hbar/(e^2A_F)$ relationship, suggesting that ρλ is determined by the Fermi surface area. (b) Parity plot comparing estimated ρλ from Fermi surface area and calculated ρλ from full electronic band structure. Data points closely follow the $y = x$ line, showing that ρλ can be well predicted from the Fermi surface area.

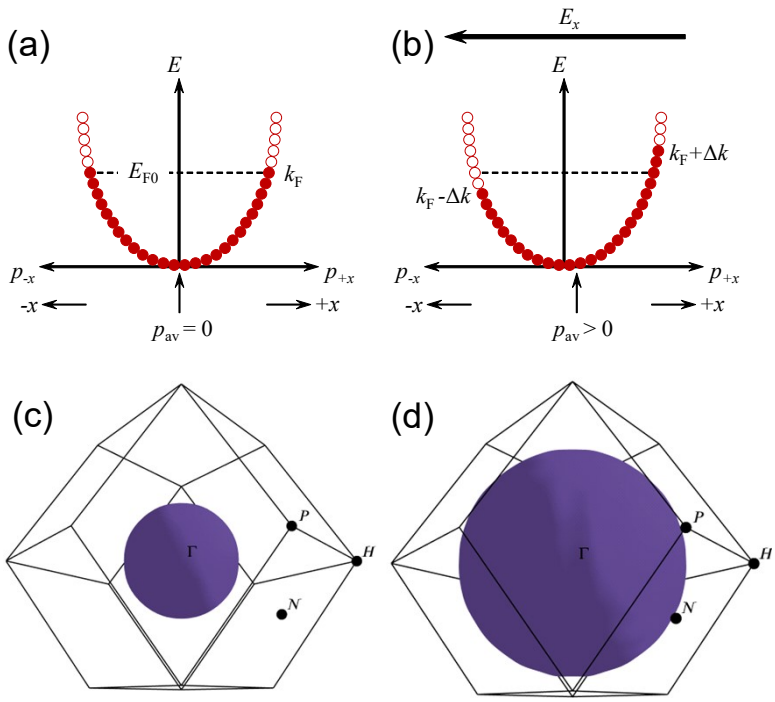

Figure S2 (a) and (b) The occupation of electronic states based on the free electron model in the (a) absence of external field and (b) presence of external field. The figures show that current flow is due to the changes in the occupancy of electronic states near the Fermi energy. (c) and (d) The Fermi surface of elemental bulk metal potassium with (c) potassium valence $v = 0.125$ and (d) potassium valence $v = 1$. Obviously, a higher valence means a higher valence electron density, which results in a larger Fermi volume and requires a larger Fermi surface area to enclose. The Brillouin zones are outlined by black lines. High symmetric k-points are also indicated.

Table S6 The crystal structure, number of valence electrons per atom v, valence electron density n_v ($\times 10^{22}$ cm^{-3}), Fermi surface area A_F predicted from n_v, calculated A_F, ρλ predicted from A_F, and calculated ρλ from full band structure for elemental bulk metals and selected 2D metals.

Metal	Crystal structure	v	n_v ($\times 10^{22}$ cm^{-3})	A_F predicted from n_v (Å^{-2})	Calculated A_F (Å^{-2})	ρλ predicted from A_F ($\times 10^{-16}$ Ω·m^2)	Calculated ρλ ($\times 10^{-16}$ Ω·m^2)	
							[100]	[001]
Cu	fcc	1	8.49	23.23	22.94	6.66	6.75	-
Ag	fcc	1	5.86	18.15	17.66	8.66	8.75	-
Al	fcc	3	17.4	37.50	30.60	5.00	5.00	-
Au	fcc	1	5.90	18.23	17.82	8.58	8.70	-
Ca	fcc	2	4.63	15.50	10.04	15.2	12.7	-
Ni	fcc	2	18.3	38.72	55.03	2.78	3.17	-
Rh	fcc	2	14.5	33.21	45.84	3.33	3.29	-
Na	bcc	1	2.55	10.42	10.71	14.3	14.0	-
K	bcc	1	1.37	6.889	6.839	22.4	22.2	-
W	bcc	2	12.6	30.30	17.36	8.81	8.50	-
Mo	bcc	2	12.8	30.55	24.02	6.36	6.15	-
Be	hcp	2	24.7	47.37	6.656	23.0	17.0	24.9
Mg	hcp	2	8.62	23.47	14.66	10.4	9.80	9.10
Zn	hcp	2	13.1	31.11	14.85	10.3	9.70	8.90
Co	hcp	2	18.1	38.49	43.04	3.55	3.90	2.44
Cd	hcp	2	9.31	24.71	11.70	13.1	12.7	12.7
Ru	hcp	2	14.4	33.07	30.87	4.95	5.14	3.91
$TiTe_2$	1T	-	-	-	6.257	24.43	17.1	-
VS_2	1T	-	-	-	11.22	13.62	12.9	-
$TaSe_2$	1T	-	-	-	9.708	15.74	12.0	-
$ZrTe_2$	1T	-	-	-	3.561	42.93	27.5	-
ReS_2	1T	-	-	-	11.40	13.41	10.0	-
$ReTe_2$	1T	-	-	-	9.048	16.89	12.4	-
$TiTe_2$	2H	-	-	-	3.341	45.76	56.0	-
VS_2	2H	-	-	-	9.382	16.29	13.6	-
$TaSe_2$	2H	-	-	-	7.850	19.47	13.5	-
$ZrTe_2$	2H	-	-	-	2.259	67.68	86.0	-
ReS_2	2H	-	-	-	5.323	28.72	22.9	-
$ReTe_2$	2H	-	-	-	5.706	26.79	16.5	-
Zr_2SnC	hex.	-	-	-	11.32	13.50	7.74	-
Ta_3InC_2	hex.	-	-	-	12.88	11.87	8.79	-
Hf_2SiC	hex.	-	-	-	13.28	11.51	8.50	-
Cr_3GeC_2	hex.	-	-	-	13.52	11.30	11.4	-
V_4AlC_3	hex.	-	-	-	13.95	10.95	9.58	-
Mo_4GaC_3	hex.	-	-	-	18.02	8.484	6.13	-

Zr_2SnN	hex.	-	-	-	8.459	18.07	10.2	-
Ta_3InN_2	hex.	-	-	-	0.837	182.6	94.6	-
Hf_2SiN	hex.	-	-	-	8.340	18.33	12.2	-
Cr_3GeN_2	hex.	-	-	-	17.53	8.721	8.22	-
V_4AlN_3	hex.	-	-	-	6.249	24.46	21.6	-
Mo_4GaN_3	hex.	-	-	-	11.50	13.29	10.1	-
TiOOH	orth.	-	-	-	9.766	15.65	33.0	-
FeOI	orth.	-	-	-	11.96	12.78	41.6	-
CeOF	orth.	-	-	-	9.903	15.43	23.4	-
MnOCl	orth.	-	-	-	14.16	10.79	11.6	-
NpOBr	orth.	-	-	-	8.166	18.72	15.6	-

Note: In the crystal structure column, we use the following abbreviation. fcc: face-centred cubic, bcc: body-centred cubic, hcp: hexagonal closed packed; 1T: trigonal and 2H: hexagonal are two common phases of TMDs; hex.: hexagonal, orth.: orthorhombic.

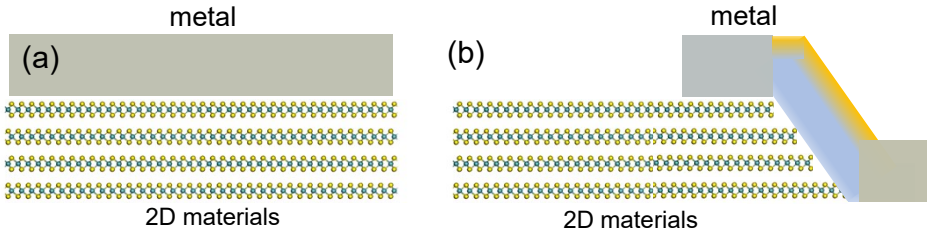

Figure S3. Schematics of metal contact to 2D materials: (a) top contact, (b) edge contact